

SUPPLEMENTAL FIGURES

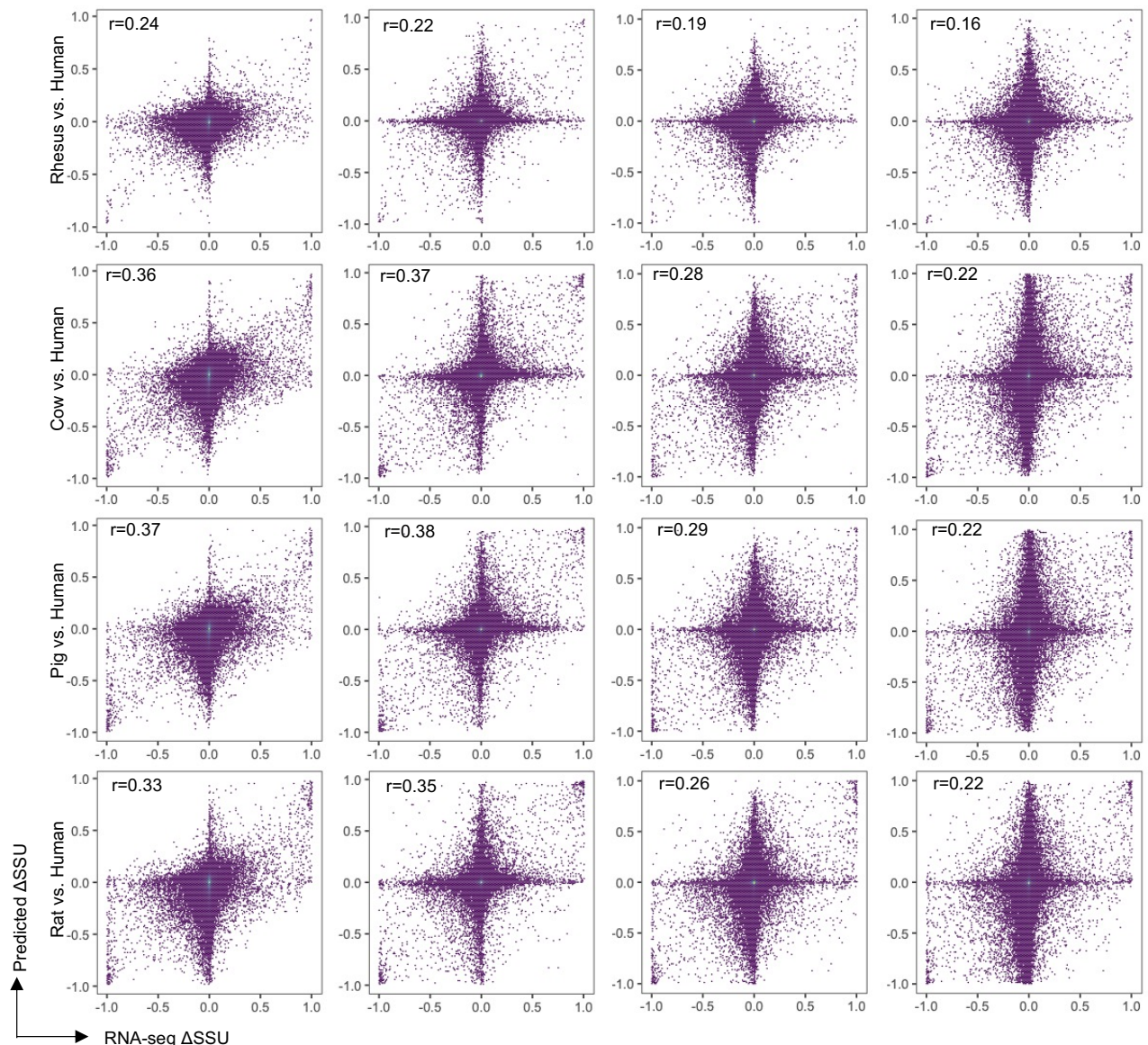


Figure S1: Distribution of predicted and experimental ΔSSU for splice sites between the other species.

Related to Fig. 4A in the main text. Distribution of ΔSSU predicted by different methods and experimental ΔSSU is shown for splice sites in additional species homologous to humans.

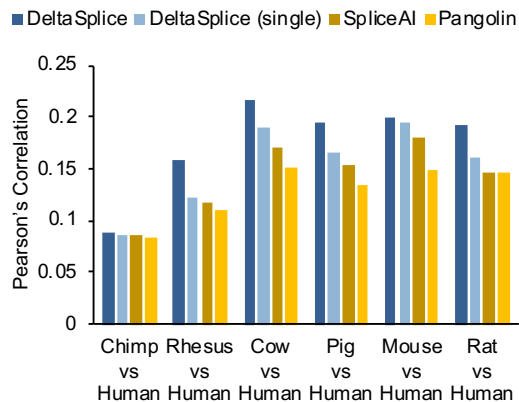
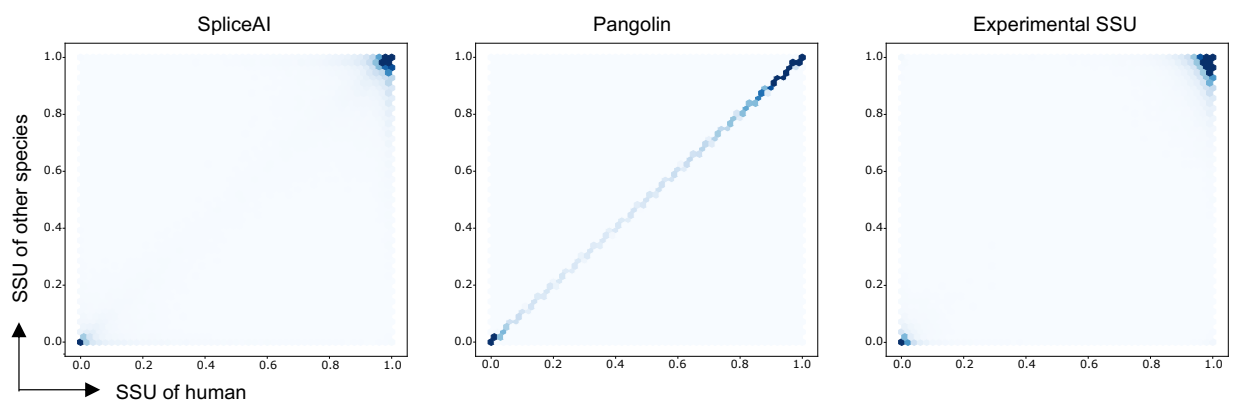
A**B**

Figure S2: Additional assessment of DeltaSplice and other methods in predicting Δ SSU of orthologous splice sites in human and other species. Related to **Fig. 2** and **Fig. 4** in the main text. **A.** Pearson correlations of predicted and RNA-seq measured Δ SSU. Similar to Fig. 4B in the main text but the correlations were calculated using orthologous splice sites with Δ SSU ≤ 0.5 between human and the other compared species. **B.** Joint distribution of SSU for orthologous splice sites in human and other species. SSU values were predicted by SpliceAI (left), Pangolin (middle), or measured by RNA-seq (right).

FAS exon 6

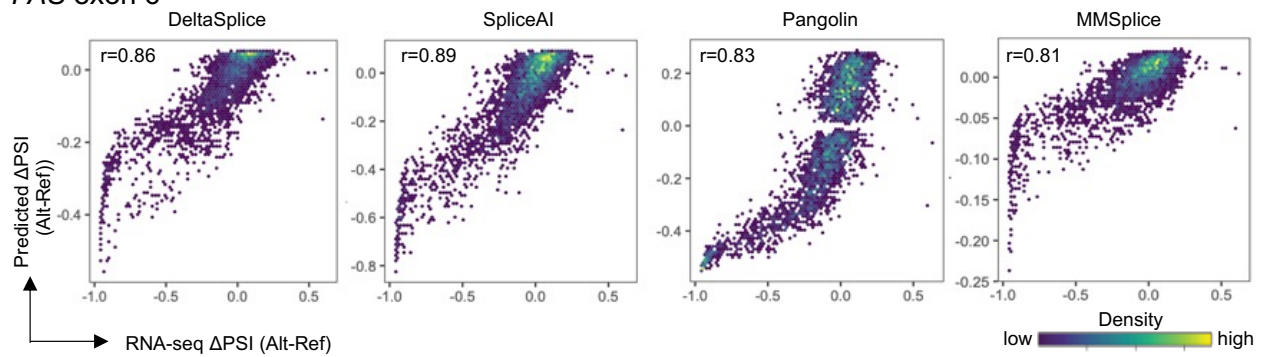


Figure S3: The performance of DeltaSplice and baseline methods in predicting splicing-altering mutations as measured by reporter assays. Similar to Fig. 5A in the main text, but for the *FAS* exon 6 dataset.

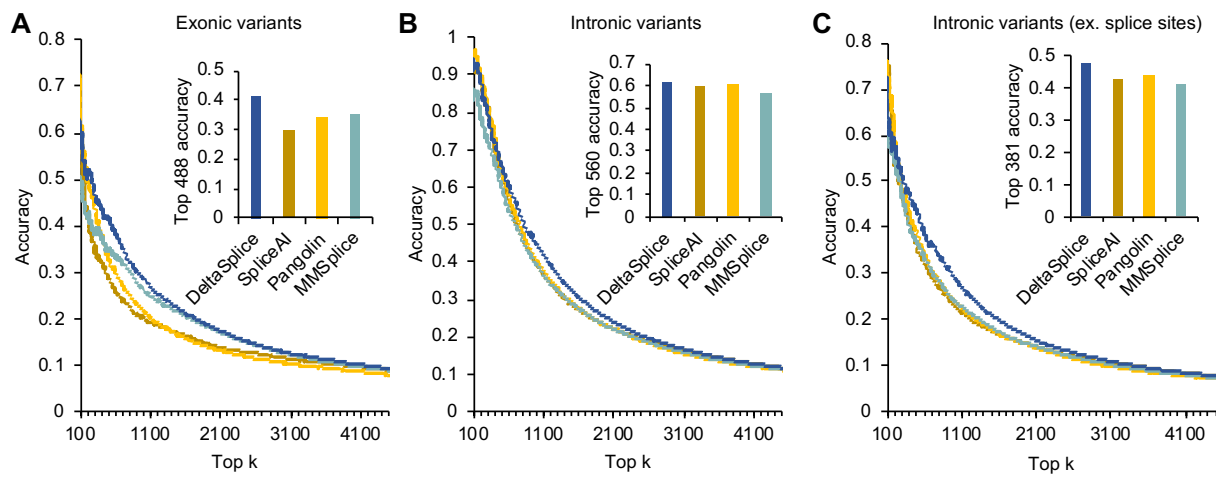


Figure S4: Performance of DeltaSplice and the other compared methods in predicting splicing-altering variants in MFASST dataset. Related to Fig. 5B,C in the main text. **A.** Exonic variants. **B.** Intronic variants including splice site mutations. **C.** Intronic variants excluding splice site mutations. See Fig. 5B,C legends for more details.

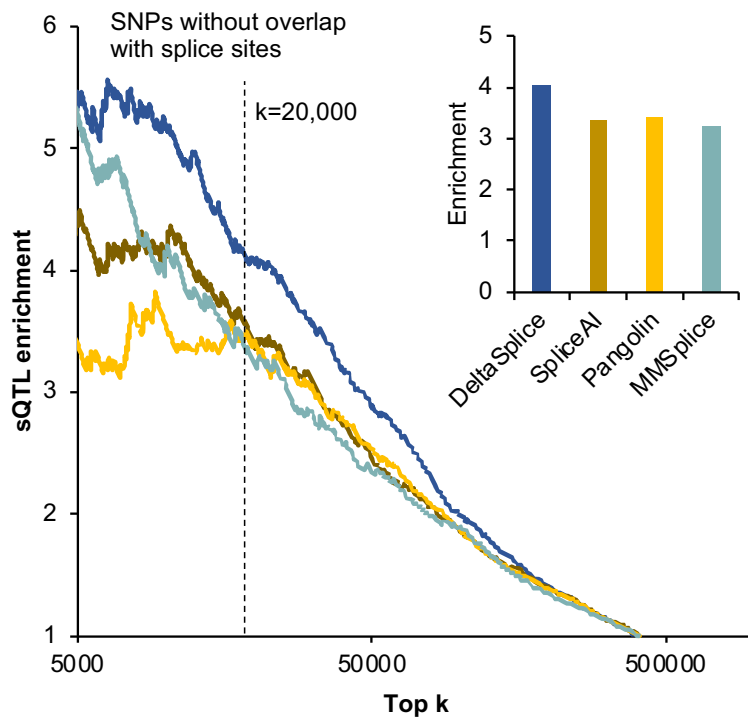


Figure S5: The performance of DeltaSplice and baseline methods in predicting splicing-altering mutations at sQTLs. Similar to Fig. 6 in the main text, but variants overlapping with splice sites were excluded for analysis.

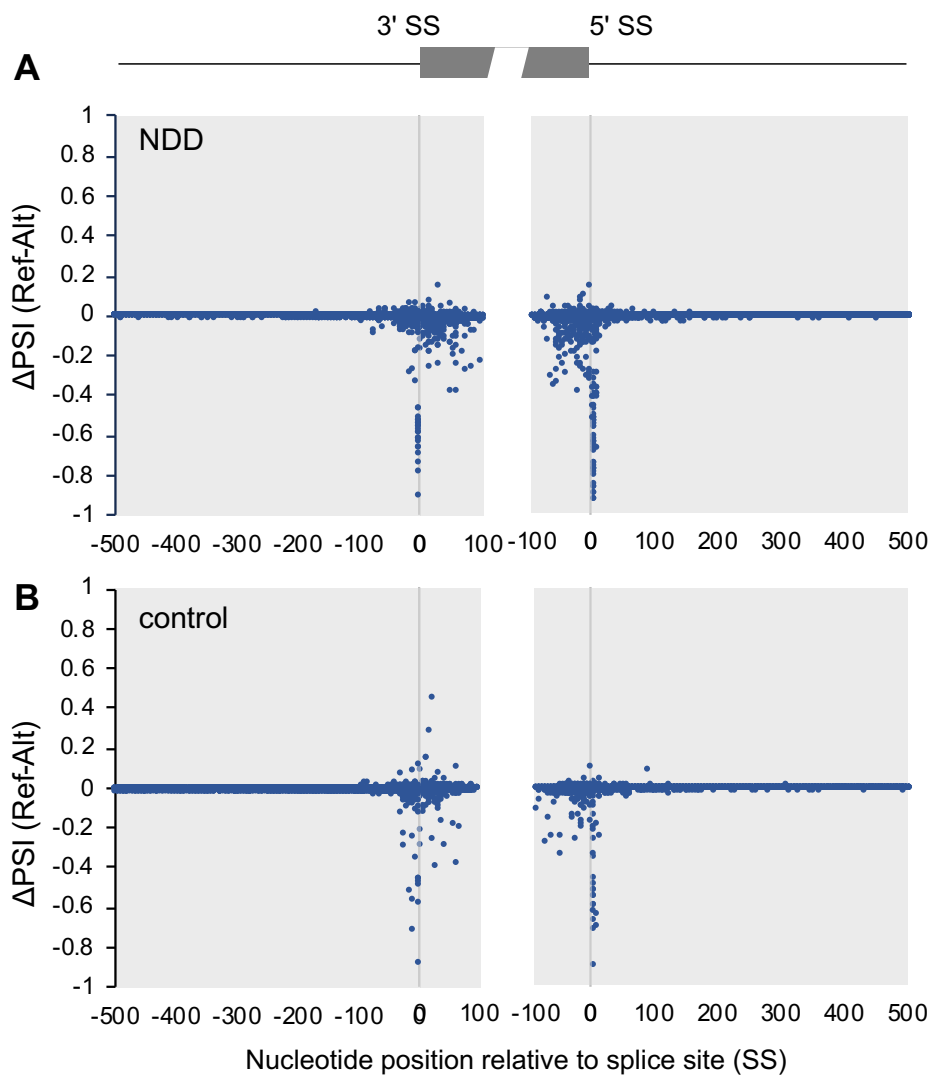


Figure S6: Predicted splicing changes caused by *de novo* mutations depending on their distance from the splice sites. Related to Fig. 7A in the main text. **A.** Autism cases. **B.** Controls. *De novo* mutations were derived from whole-genome sequencing.

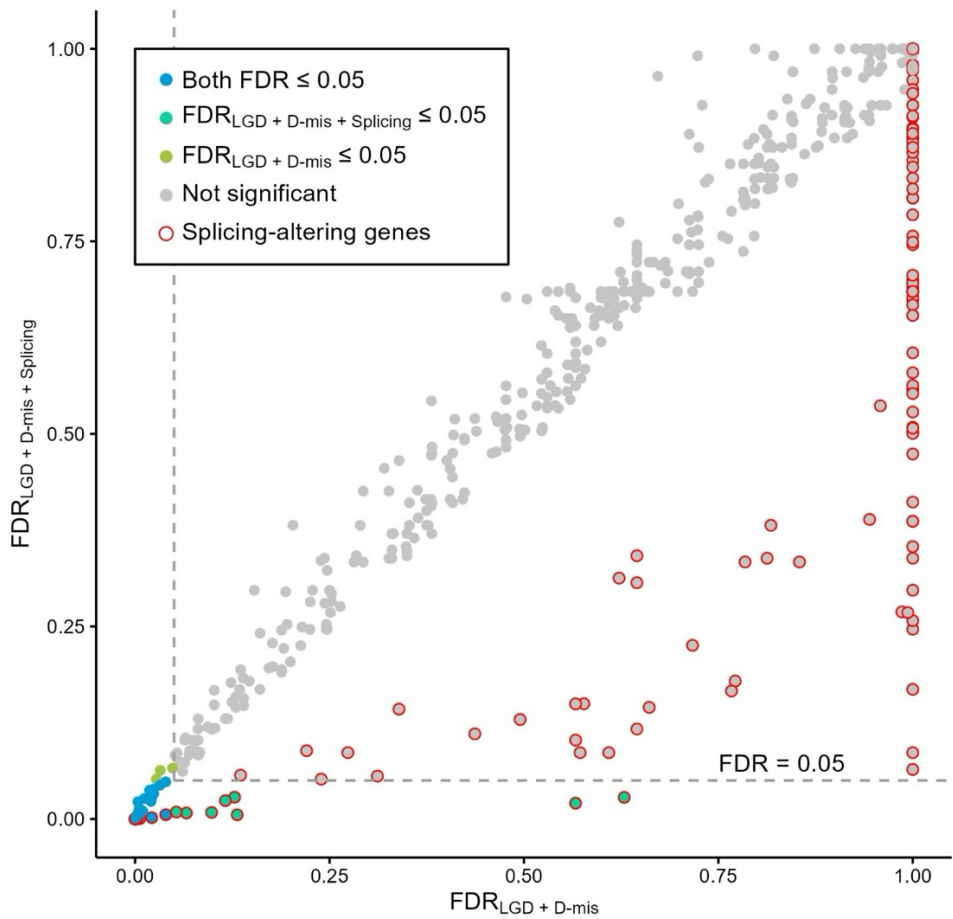


Figure S7: Distribution of FDR values of all genes. FDRs were generated using two models (model 1: LGD + D-mis, model 2: LGD + D-mis + splicing, see Methods). The gray dashed line indicates the significant threshold. Genes carrying predicted splicing-altering mutations were labeled with red circles.